PLOS | ONE

RESEARCH ARTICLE

Numerical Simulation of CO_2 Flooding of Coalbed Methane Considering the Fluid-Solid Coupling Effect

Jianjun Liu[1,2], Guang Li[1,2]*, Yue Zhang[3]

1 School of Geoscience and Technology, Southwest Petroleum University, Chengdu, China, **2** State Key Laboratory of Oil and Gas Reservoir Geology and Exploitation, Southwest Petroleum University, Chengdu, China, **3** Jidong Oilfield Company, PetroChina, Tangshan, Hebei, China

* li_1616@163.com

Citation: Liu J, Li G, Zhang Y (2016) Numerical Simulation of CO_2 Flooding of Coalbed Methane Considering the Fluid-Solid Coupling Effect. PLoS ONE 11(3): e0152066. doi:10.1371/journal.pone.0152066

Editor: Jie Zheng, University of Akron, UNITED STATES

Received: December 22, 2015

Accepted: March 8, 2016

Published: March 31, 2016

Data Availability Statement: All relevant data are within the paper.

Funding: The research is financially supported by National Natural Science Foundation of China (Grant No. 51174170) and the National Science and Technology Support Program Project (Grant No. 2012BAC26B05). Jianjun Liu received the funding. The funders had no role in study design, data collection and analysis, decision to publish, or preparation of the manuscript.

Competing Interests: Although the third author is employed by a commercial company, this does not

Abstract

CO_2 flooding of coalbed methane (CO_2-ECBM) not only stores CO_2 underground and reduces greenhouse gas emissions but also enhances the gas production ratio. This coupled process involves multi-phase fluid flow and coal-rock deformation, as well as processes such as competitive gas adsorption and diffusion from the coal matrix into fractures. A dual-porosity medium that consists of a matrix and fractures was built to simulate the flooding process, and a mathematical model was used to consider the competitive adsorption, diffusion and seepage processes and the interaction between flow and deformation. Due to the effects of the initial pressure and the differences in pressure variation during the production process, permeability changes caused by matrix shrinkage were spatially variable in the reservoir. The maximum value of permeability appeared near the production well, and the degree of rebound decreased with increasing distance from the production well.

Introduction

The porosity and permeability of fracture systems in coalbed methane reservoirs are influenced by effective stress and gas adsorption-desorption. In 1987, Gray put forward that when the coalbed methane desorbs, the coal matrix shrinks, which can cause crack expansion and permeability increases [1]. In 1998, Mavor used observational data from the San Juan Basin to prove the coal matrix shrinkage hypothesis [2]. In the same year, Palmer and Mansoori derived the permeability calculation formula (P&M formula), which considers the effects of effective stress and matrix shrinkage on permeability. Based on this formula, they studied the actual production process of the San Juan Basin and successfully explained the "gas production rebound" phenomenon [3]. At present, many scholars have performed numerous studies on experimental and theoretical aspects. Jessen [4] reported a mixed gas injection mechanism based on research on the different effects associated with enhancing recovery efficiency using injected CO_2, N_2 and mixed gases. Karacan [5] found that adsorption and swelling phenomena

in coal were heterogeneous and different parts of a coal sample behave differently. Gensterblum [6] reported that there were three relationships between coal swelling and the amount of CO_2 adsorbed by coal and that coal swelling was not affected at pressures below a few atmospheres. An [7] carried out an experimental and numerical investigation on anisotropic permeability of coal and evaluated the effects of the anisotropic permeability variation on CO_2-ECBM. Kumar [8] investigated the evolution of permeability heterogeneity during CO_2-ECBM. Alexej [9] analyzed the effect of moisture on sorption capacity for coals of different rank and the competitive CO_2/CH_4 sorption behavior in binary gas mixtures by using laboratory experiment method. Massarotto [10] researched the changes in reservoir properties from injection of supercritical CO_2 into coal seams. In addition, deformations induced by adsorption were studied by the researchers [11–14]. However, those studies of CO_2 flooding of coalbed methane mostly focus on competitive adsorption between CO_2 and CH_4, gas-water two-phase flow and the effect caused by coal or rock deformation on permeability. Very little research has been conducted on the dynamic evolution of permeability during CO_2 injection.

In this paper, based on the existing theory and test results [15–20], a mathematical model considered competitive adsorption, diffusion and seepage process and the interaction between flow and deformation was established, using software simulated the production situation of CO_2 flooding, emphasis analyses the dynamic evolution of permeability during the process of CO_2 flooding.

Mathematical Model of CO_2 Flooding of Coalbed Methane

Model assumptions: Both the coalbed methane and water flow under Darcy flow, and the two-phase fluid flow can be expressed as follows:

$$\frac{\partial}{\partial x}\left[\frac{k_{rg}k_x}{B_g\mu_g}\left(\frac{\partial p_g}{\partial x}-\rho_g g\frac{\partial D}{\partial x}\right)\right]+\frac{\partial}{\partial y}\left[\frac{k_{rg}k_y}{B_g\mu_g}\left(\frac{\partial p_g}{\partial y}-\rho_g g\frac{\partial D}{\partial y}\right)\right]+\frac{\partial}{\partial z}\left[\frac{k_{rg}k_z}{B_g\mu_g}\left(\frac{\partial p_g}{\partial z}-\rho_g g\frac{\partial D}{\partial z}\right)\right]+q_f-q_g=\frac{\partial}{\partial t}(\phi\rho_g S_g) \tag{1}$$

$$\frac{\partial}{\partial x}\left[\frac{k_{rw}k_x}{B_w\mu_w}\left(\frac{\partial p_w}{\partial x}-\rho_w g\frac{\partial D}{\partial x}\right)\right]+\frac{\partial}{\partial y}\left[\frac{k_{rw}k_y}{B_w\mu_w}\left(\frac{\partial p_w}{\partial y}-\rho_w g\frac{\partial D}{\partial y}\right)\right]+\frac{\partial}{\partial z}\left[\frac{k_{rw}k_z}{B_w\mu_w}\left(\frac{\partial p_w}{\partial z}-\rho_w g\frac{\partial D}{\partial z}\right)\right]-q_w=\frac{\partial}{\partial t}(\phi\rho_w S_w) \tag{2}$$

where k_{rg} is the relative gas permeability; k_{rw} is the relative water permeability; k_x, k_y, and k_z are the absolute permeabilities in the X, Y, and Z directions, respectively; ρ_g is the gas density; ρ_w is the water density; g is the acceleration of gravity, m/s^2; P_g is the gas pressure, MPa; P_w is the water pressure, MPa; S_g is the gas saturation; S_w is the water saturation; ϕ is porosity; D is standard height, m; μ_g is the viscosity of the gas; μ_w is the viscosity of the water; B_g is the formation volume factor of the gas; B_w is the formation volume factor of the water; q_f is the amount of gas in the fracture due to the diffusion effect; q_g is the source term of the gas, m^3/d; and q_w is the source term of the water, m^3/d.

Permeability in coals is a function of effective stress and matrix shrinkage. The calculation uses the P&M equation (Palmer and Mansoori 1998 [3]), which is expressed as follows:

$$\frac{\phi_f}{\phi_{f0}}=1+C_f(P-P_i)+\xi_L\left(1-\frac{K}{M}\right)\left(\frac{P_i}{P_i+P_L}-\frac{P}{P+P_L}\right) \tag{3}$$

In Eq (3), the central part indicates the influence of stress change (cleat deformation) on porosity, the latter part indicates the influence of matrix shrinkage on porosity, when considers only cleat deformation, the expression can be expressed as Eq (4):

$$\frac{\phi_f}{\phi_{f0}} = 1 + C_f(P - P_i) \tag{4}$$

$$\frac{k_f}{k_{f0}} = \left(\frac{\phi_f}{\phi_{f0}}\right)^3 \tag{5}$$

where $C_f = \frac{1}{\phi_0 M}$; $\frac{K}{M} = \frac{1}{3}\left(\frac{1+\mu}{1-\mu}\right)$; $M = E\frac{1-\mu}{(1+\mu)(1-2\mu)}$

ϕ_f is the fracture porosity at pressure p; ϕ_{f0} is the initial natural fracture porosity at a given pressure; C_f is the pore volume compression coefficient, 1/kPa; ξ_L is the strain at infinite pressure; K is the bulk modulus, kPa; M is the axial modulus, kPa; P_i is the initial pressure, kPa; K_{f0} is the initial permeability, E is the elasticity modulus, kPa; and μ is Poisson's ratio; ϕ_0 is the initial porosity, C_f is rock compressibility.

Assuming that the absorption behaviors of CH_4 and CO_2 in coal follow the rule of Langmuir, the amount of adsorbed gas can be expressed as follows:

$$V_i = \frac{(V_m)_i b_i p_i}{1 + \sum_{j=1}^{n} b_j p_j} \tag{6}$$

where $(V_m)_i$ is the adsorption constant of the pure species gas i, cm^3/g; b_i is the pressure-constant of the pure species gas i, 1/MPa; and p_i is the partial pressure of gas component i, MPa.

Coalbed methane diffuses from the matrix to fractures following Fick's law:

$$\frac{\partial C}{\partial t} = \frac{\partial^2 C}{\partial X^2} \tag{7}$$

where C is the gas concentration, mol/m, and X is the distance of gas diffusion, m.

The convection diffusion equation for gas can be written as follows:

$$\frac{\partial}{\partial t}(\phi(p)C) + \nabla(-D(\mu) + C\mu) = 0 \tag{8}$$

where u is the pore velocity of fluid, m/s, and D is the tensor diffusion, m^2/s.

The capillary pressure equation and the saturation equation can be written, respectively as follows:

$$P_c = P_g - P_w \tag{9}$$

$$S_g + S_w = 1 \tag{10}$$

where P_c is the capillary pressure, Pa.

Numerical Simulation of CO_2 Flooding of Coalbed Methane

A commercial reservoir simulator was used in this study (CMG-GEM, 2012). The well location distribution is shown in Fig 1. The model used closed boundaries and the change of temperature was not considered in our study. CO_2 was injected using a constant rate of 2000 m^3/d. (at surface condition) for a period of 1940 days. Relevant parameters are provided in Table 1.

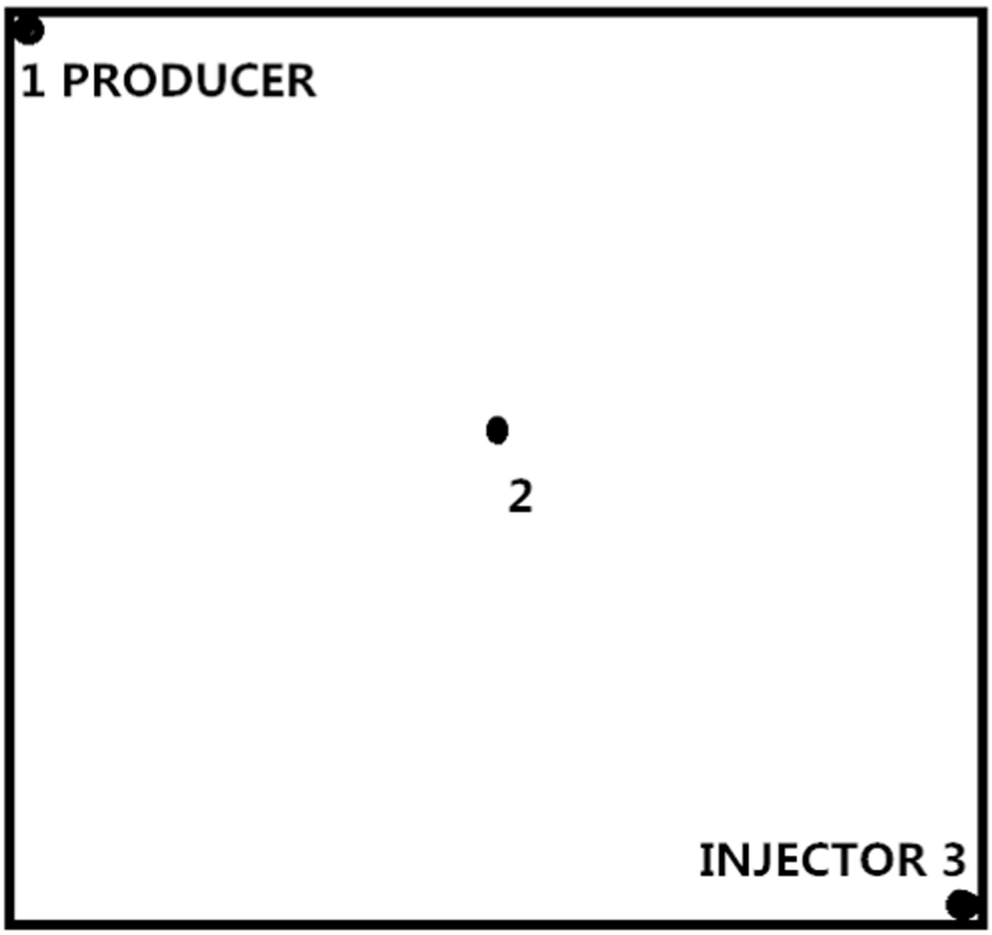

Fig 1. Well location.

doi:10.1371/journal.pone.0152066.g001

Fig 2 compares the two permeability models used in the simulation. A significant difference in permeability changes is present between the two models. The effect on permeability caused by matrix shrinkage appears when the reservoir pressure reaches a low level (approximately 3.5 MPa), and becomes more significant with further drops in reservoir pressure.

Table 1. Selected parameters.

Parameters	Value	Parameters	Value
Gridding	40*40*1	**Reservoir temperature (°C)**	45
Grid spacing (m)	5 5 9	**Reservoir pressure (MPa)**	7.65
Young's modulus of elasticity (kPa)	3000000	**Top depth (m)**	900
Matrix porosity (%)	0.5	**Cleat porosity (%)**	0.1
Poisson ratio	0.4	**CO_2/CH_4 Langmuir pressure (kPa)**	1090/350
CO_2/CH_4 Diffusion value (d)	100/100	**Cleat permeability (mD)**	4.0
Coal compression coefficient (kPa^{-1})	1.45E-7	**Coal density (kg/m^3)**	1400
CO_2 maximum adsorption capacity by unit mass (mol/kg)	1.0	**CH_4 maximum adsorption capacity by unit mass (mol/kg)**	0.5

doi:10.1371/journal.pone.0152066.t001

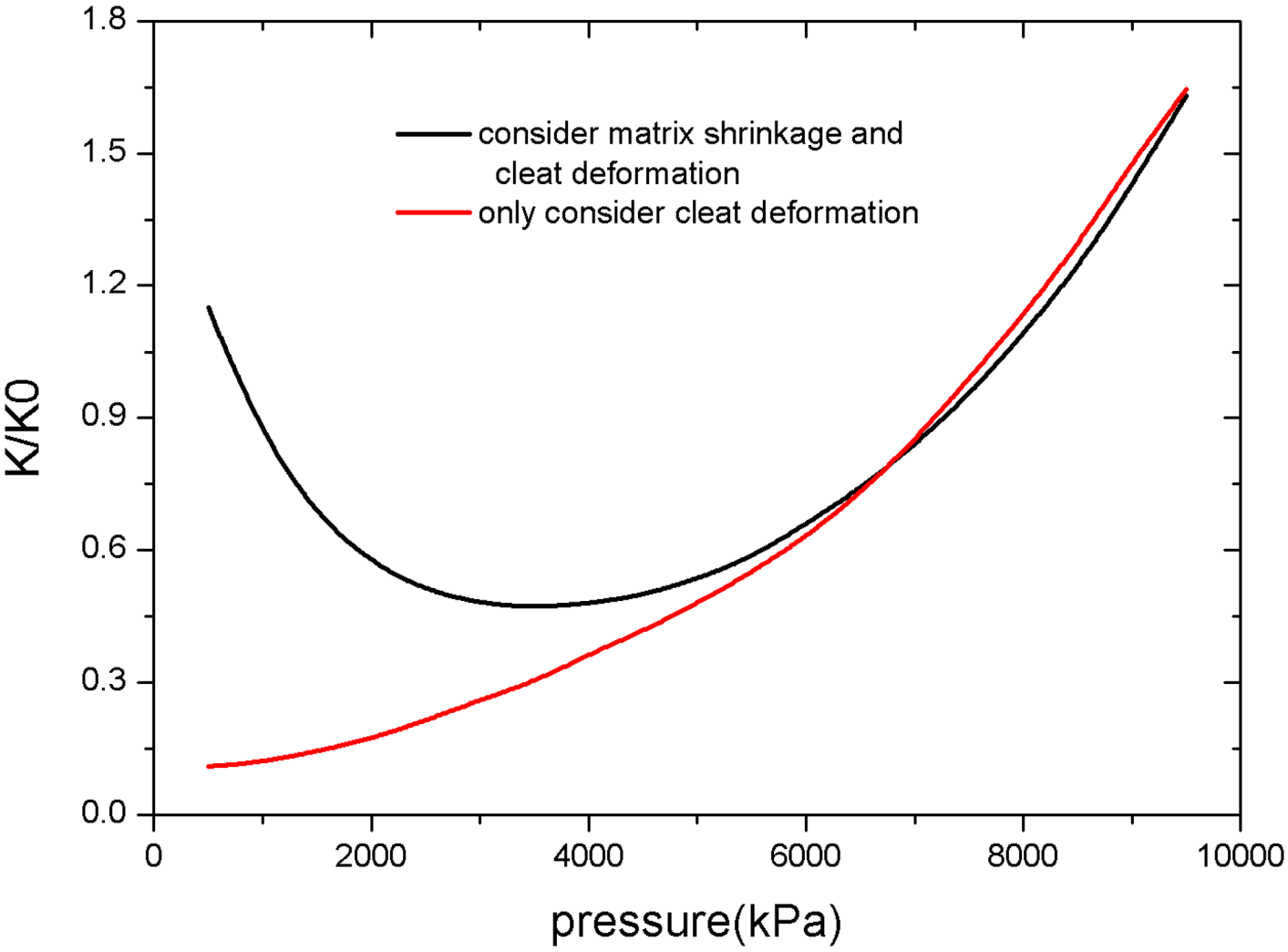

Fig 2. Permeability models used in the simulation.

doi:10.1371/journal.pone.0152066.g002

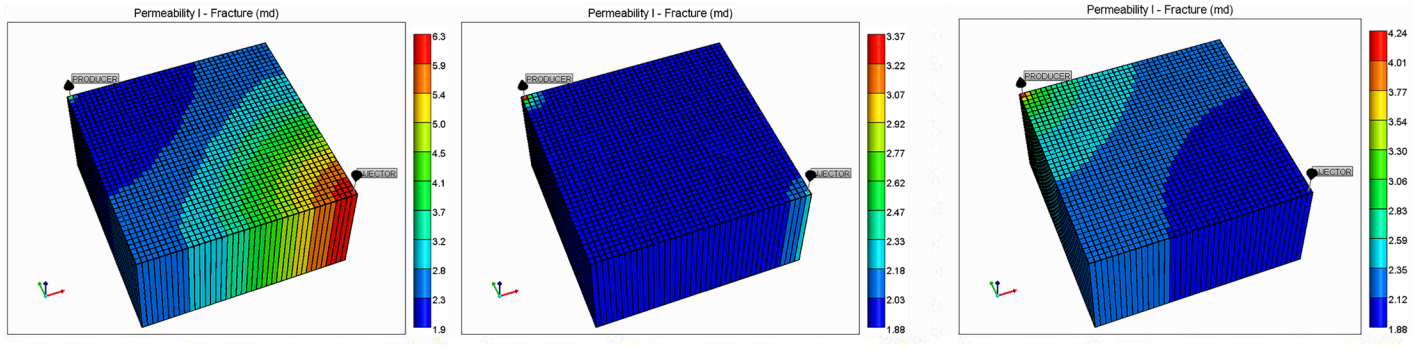

(a) Injecting CO_2 for 30 days. (b) Injecting CO_2 for 150 days. (c) Injecting CO_2 for 1940 days.

Fig 3. Permeability distribution in the reservoir considering both matrix shrinkage and cleat deformation.

doi:10.1371/journal.pone.0152066.g003

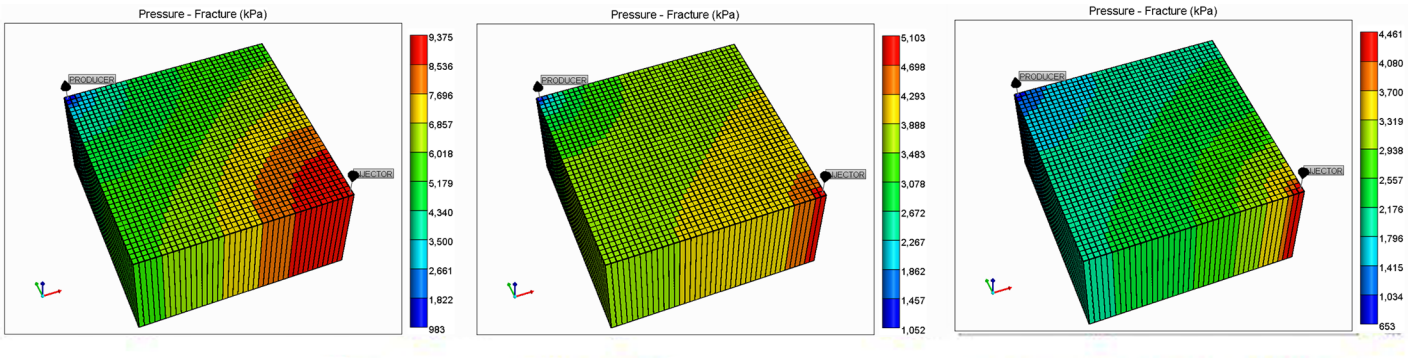

(a) Injecting CO_2 for 30 days. (b) Injecting CO_2 for 150 days. (c) Injecting CO_2 for 1940 days.

Fig 4. Pressure distribution in the reservoir considering both matrix shrinkage and cleat deformation.

doi:10.1371/journal.pone.0152066.g004

To validate the effects of matrix shrinkage on fracture permeability, two different permeability equations were used in the simulation. One considers both cleat deformation and matrix shrinkage, and the other considers only cleat deformation. Fig 3 shows the permeability distribution in the reservoir at various simulation times under conditions of both matrix shrinkage and crack deformation. To improve calculation speed and save calculation time, the grids used in the simulation are limited. This results in distribution contours that are not very smooth, but it does not affect the accuracy of the simulation. Because the permeability changes are affected by reservoir pressure, Fig 4 shows the pressure distribution of the reservoir at various simulation times.

The points 1, 2, and 3 in Fig 1 (point 1 is near the production well, point 2 is in the middle of the reservoir, and point 3 is near the injection well) are selected to analyze the pressure and permeability data at different times, resulting in the curves in Figs 5–10.

The value of permeability at point 1 during the whole simulation period is shown in Fig 6. At the beginning of the simulation, the reservoir pressure near the wellbore rapidly decreases to less than 3.5 MPa (Fig 5), and the permeability near the wellbore appears to rebound due to matrix shrinkage. At low drawdown pressures, the degree of permeability rebound is greater. One interpretation of this pattern is that matrix shrinkage increases pore volume, leading to an increase in permeability. In a simulation of 1,940 days, the maximum value of permeability around the production well increased to 4.3 mD, exceeding the initial permeability in the reservoir. Fig 6 shows a typical permeability curve near the production well at various periods when permeability is influenced only by cleat deformation. As the output of CH_4 and pore pressure decrease, the effective stress increases and cracks are compressed. This process makes the fluid pathways smaller and leads to a decrease in permeability.

Fig 8 presents the changes in permeability in the middle of the reservoir at various times. Because the pressure decrease was weaker than that of the area near the production well, the permeability rebound was not large, and the final value was less than 3 mD. However, the permeability still increased by 1.5 mD more than the permeability in the case in which the fracture permeability formula does not consider matrix shrinkage.

As a result of CO_2 injection, the pressure of the reservoir was replenished, slowing the pressure decrease in the reservoir, especially near the injection well where the pressure was maintained at a high value (Fig 4). The permeability in these areas consistently decreased, and the permeability curve was similar to the case that only considers cleat deformation (Fig 10).

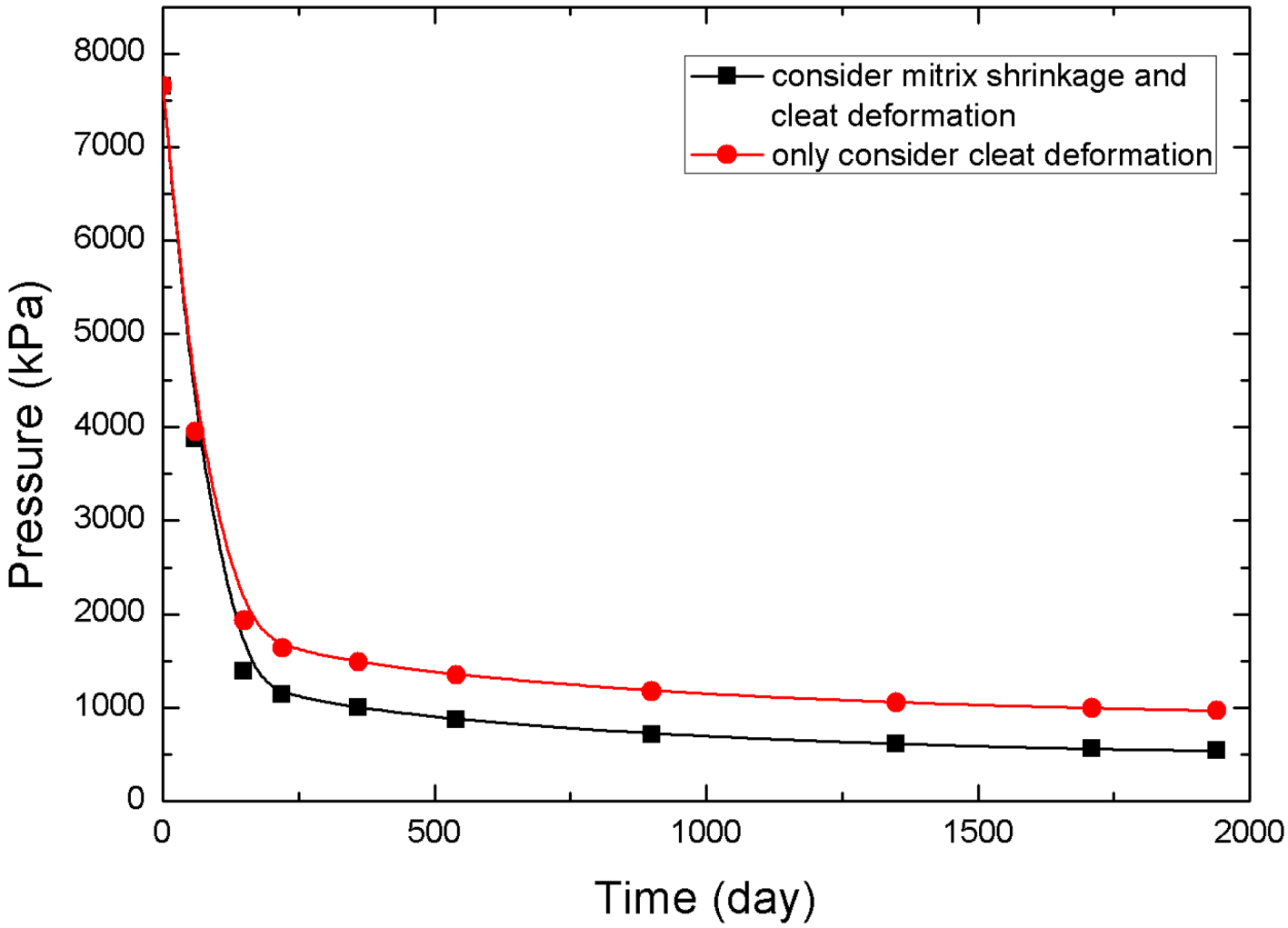

Fig 5. Pressure change curve at point 1.

doi:10.1371/journal.pone.0152066.g005

Fig 11 compares the daily gas rates of both cases to analyze the effects of matrix shrinkage on CO_2 flooding of coalbed methane (CO_2-ECBM). The peak value of daily gas rate was higher when matrix shrinkage is considered, resulting in a maximum value of 4182 m^3/day, which is 30.77% higher than that of the case that only considers cleat deformation. In the late stage of the simulation, low gas saturation becomes the main factor limiting the daily gas rate. After a simulation length of 1,700 days, the daily gas rate drops below that of the case that only considers cleat deformation. Therefore, matrix shrinkage improves the fracture permeability, thereby increasing CH_4 production during the early stages and decreasing gas saturation during the later stages.

The evolution of the cumulative production of CH_4 is shown in Fig 12. The curve clearly indicates that matrix shrinkage promotes the CO_2-ECBM process. Matrix shrinkage allows fracture permeability to increase and accelerates the output of gas. Under the given conditions in this study, the cumulative production of CH_4 was 2.25×10^6 m^3, and the recovery was 80.3%, which was 18.1% higher than the case that did not consider matrix shrinkage.

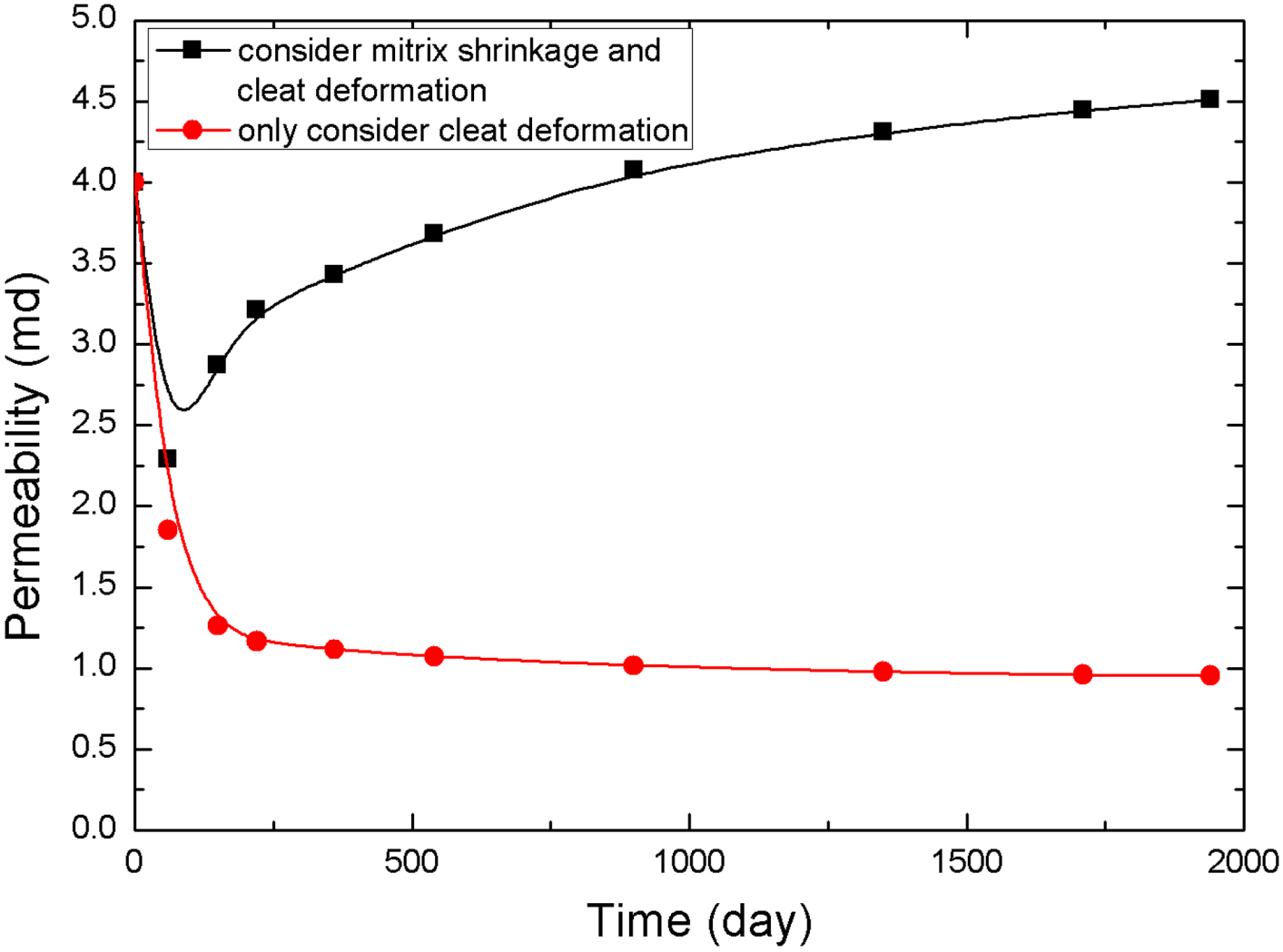

Fig 6. Permeability change curve at point 1.

doi:10.1371/journal.pone.0152066.g006

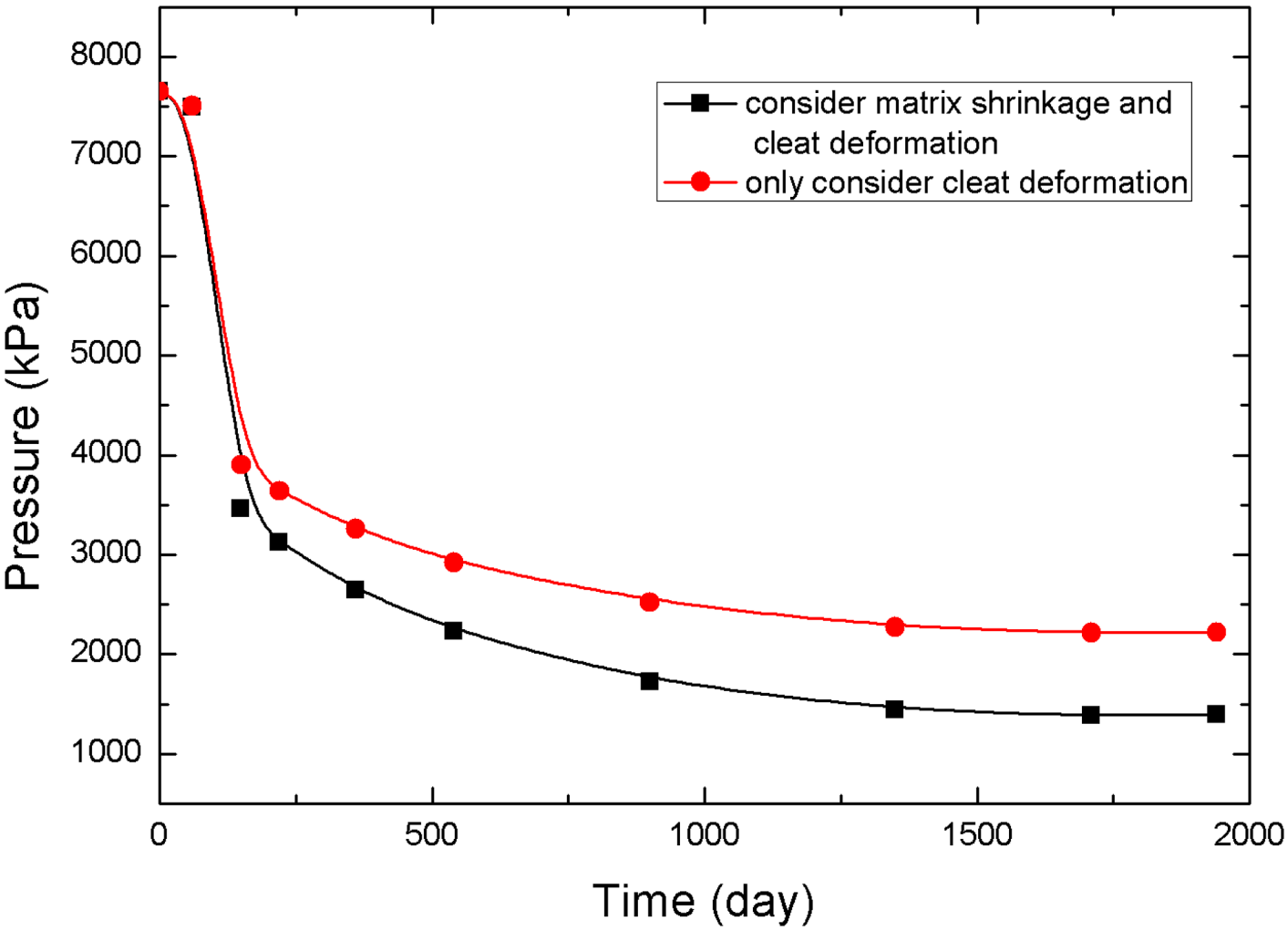

Fig 7. Pressure change curve at point 2.

doi:10.1371/journal.pone.0152066.g007

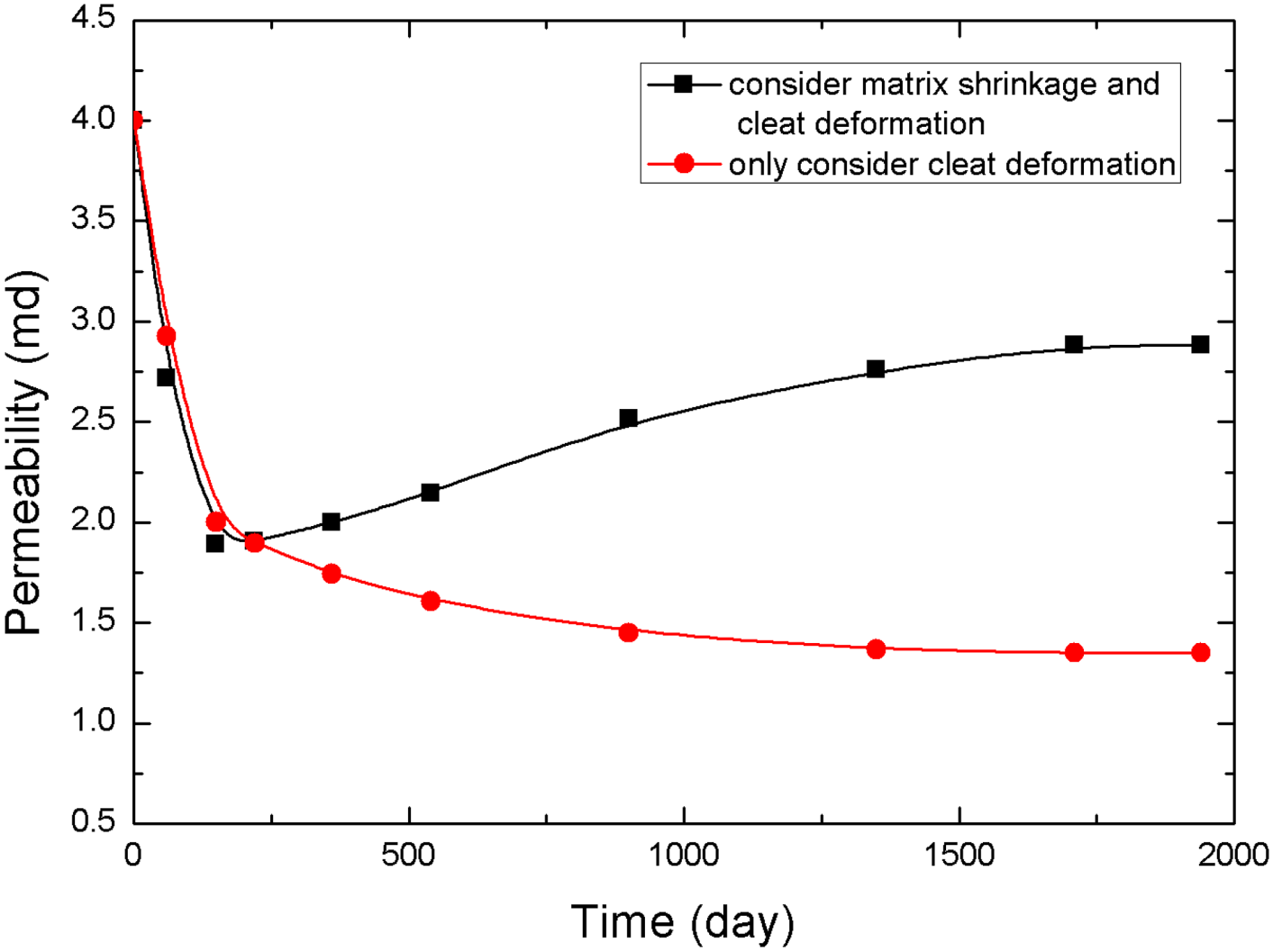

Fig 8. Permeability change curve at point 2.

doi:10.1371/journal.pone.0152066.g008

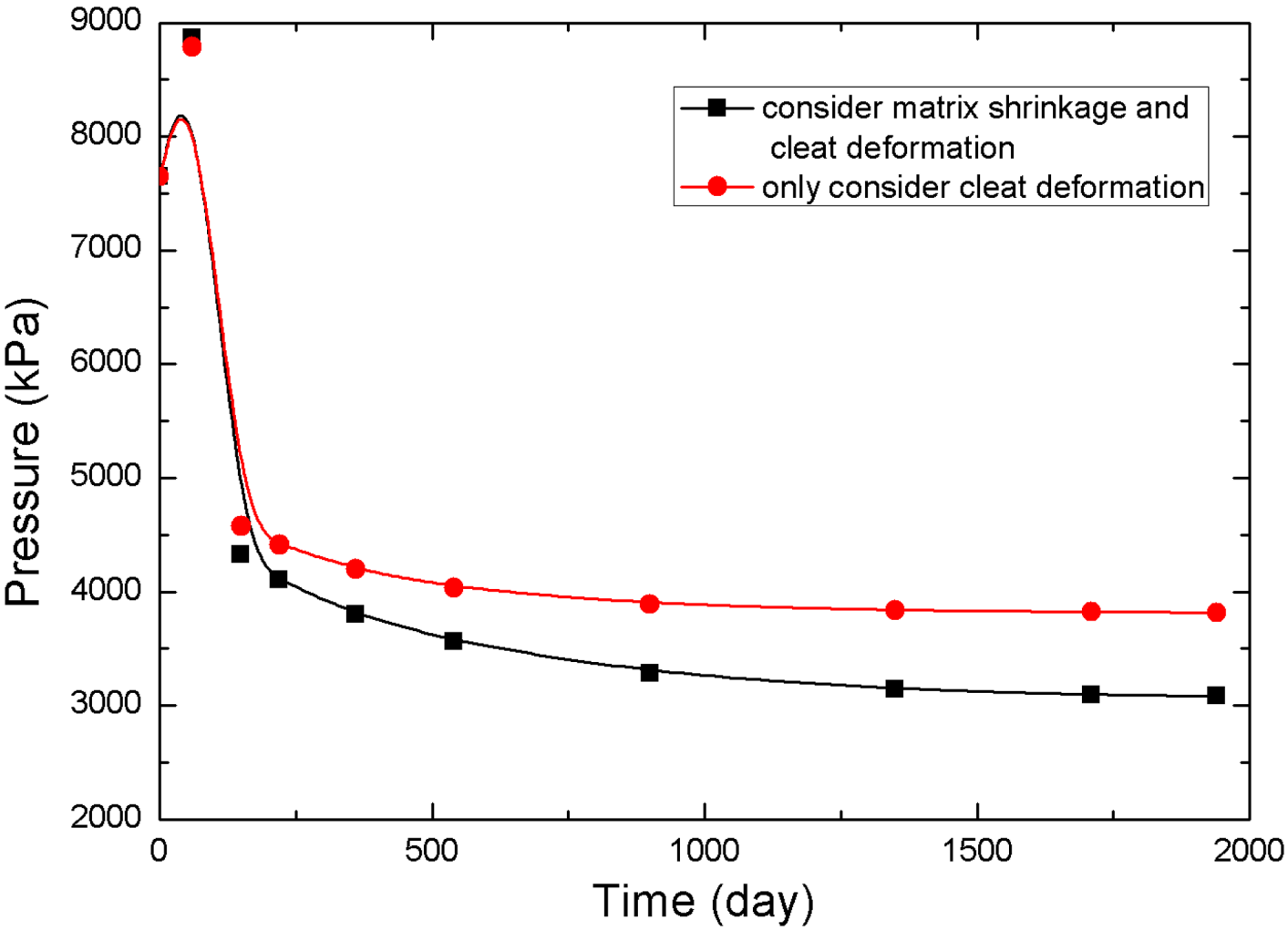

Fig 9. Pressure change curve at point 3.

doi:10.1371/journal.pone.0152066.g009

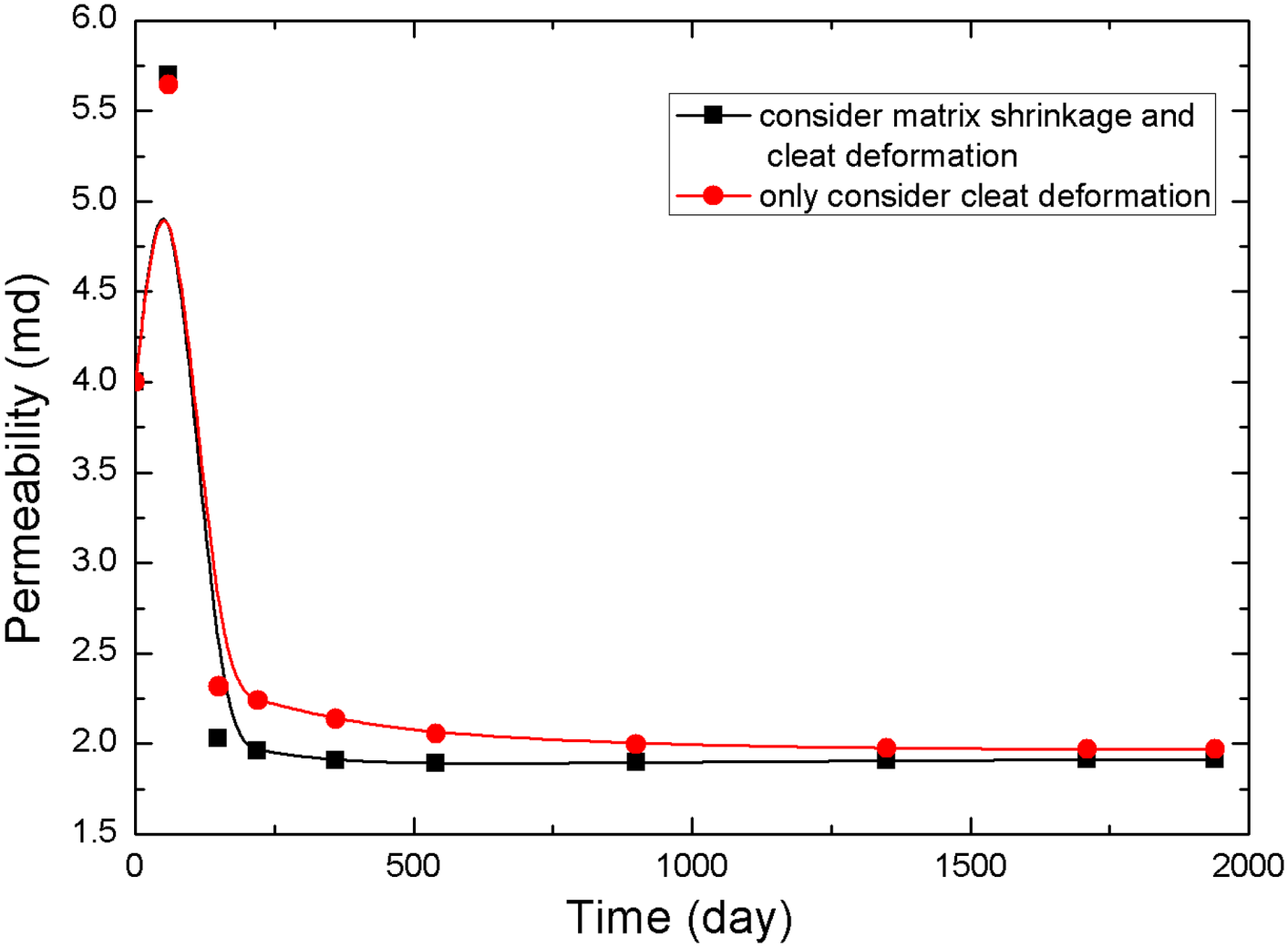

Fig 10. Permeability change curve at point 3.

doi:10.1371/journal.pone.0152066.g010

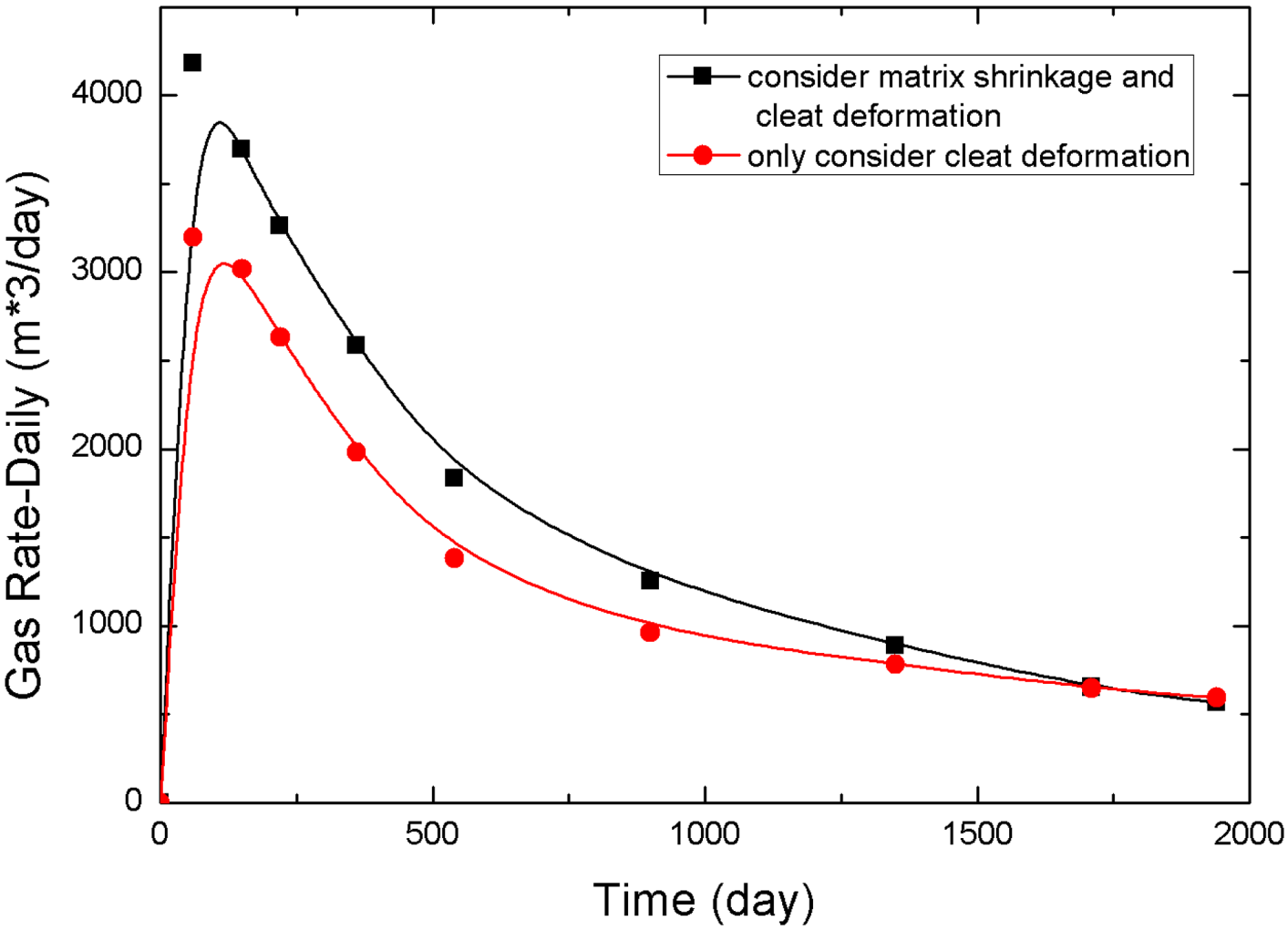

Fig 11. Comparison of daily gas rate.

doi:10.1371/journal.pone.0152066.g011

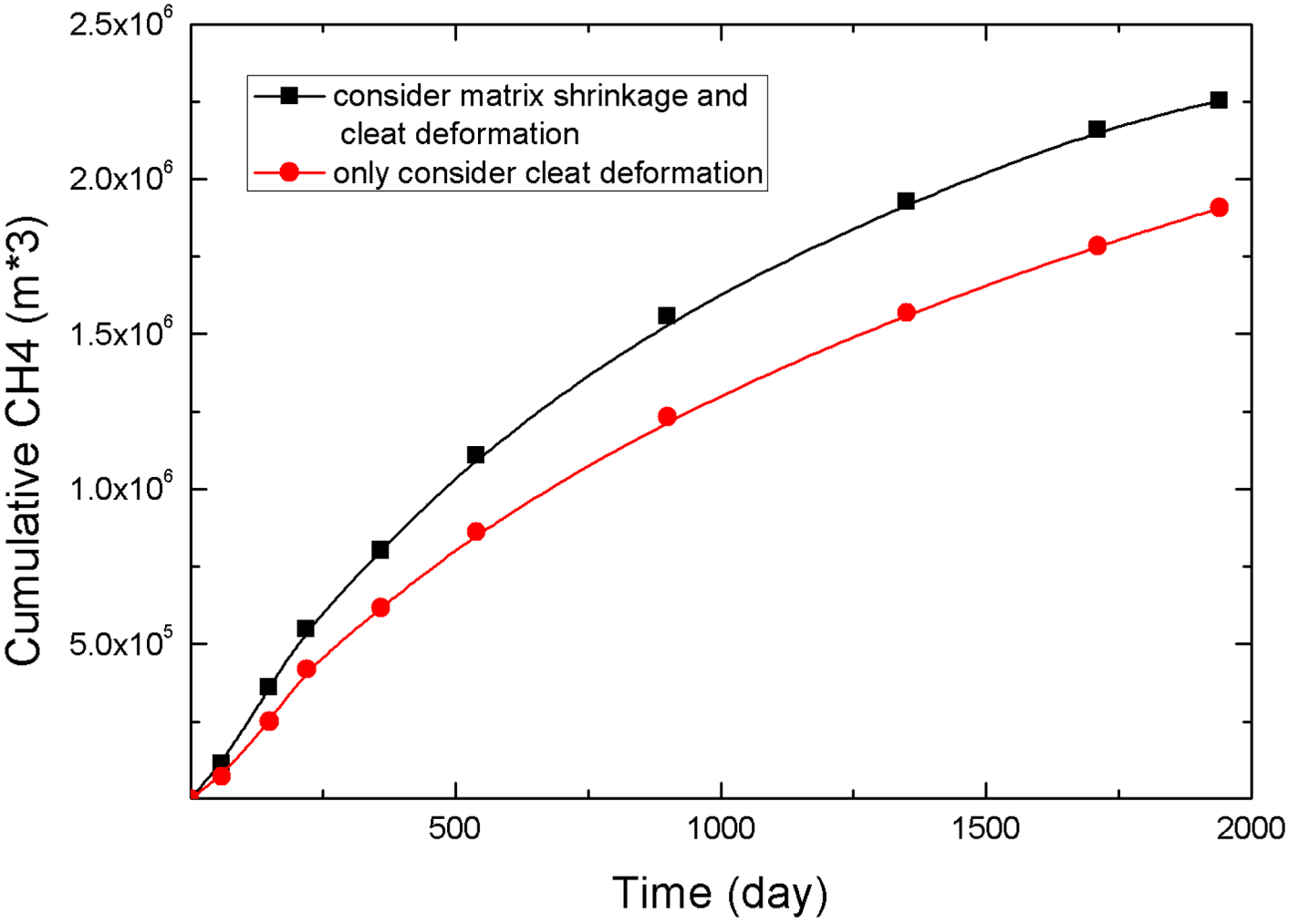

Fig 12. Comparison of cumulative production.

doi:10.1371/journal.pone.0152066.g012

Conclusions

A coupled mathematical model of CO_2 flooding that considers coal or rock deformation and multi-physical processes (competitive adsorption, convection-diffusion, seepage) was established in this paper. Using the simulation software to solve the coupling model, our study emphasized the influence of coal matrix shrinkage on permeability during CO_2 flooding. The conclusions have been reached:

1. Based on the initial pressure and the differences in pressure variations during the production process, the permeability changes caused by matrix shrinkage are spatially variable in the reservoir. The maximum permeability value appears near the production well, and the degree of rebound decreases with increasing distance from the production well.
2. Under the conditions of our study, matrix shrinkage has an galvanizing effect on CO_2-ECBM and increases the daily gas rate during the early production phase. Although the CH_4 saturation is lower in later stages, resulting in lower daily gas rates, the overall final yield is greater.
3. In general, permeability in coals is a function of pressure drawdown. In the CO_2-ECBM process, CO_2 injection changes the distribution of pressure, which changes the permeability in the reservoir. Therefore, selecting the appropriate well spacing and injection rate based on different reservoir characteristics is necessary to ensure that the CO_2 injection will not reduce the permeability of the reservoir and to achieve the optimal effects of CO_2 displacement.

Acknowledgments

The research is financially supported by National Natural Science Foundation of China (Grant No. 51174170) and the National Science and Technology Support Program Project (Grant No. 2012BAC26B05).

Author Contributions

Conceived and designed the experiments: GL. Performed the experiments: GL. Analyzed the data: GL. Contributed reagents/materials/analysis tools: JL. Wrote the paper: GL. Assisted in the numerical simulation: YZ. Gave suggestions when analyzing data: YZ.

References

1. Gray I. Reservoir engineering in coal seams: Part 1. The physical process of gas storage and movement in coal seams. SPE Reserv Eval Eng. 1987; 2: 28–34.
2. Mavor MJ, Vaughn JE. Increasing coal absolute permeability in the San Juan Basin fruitland formation. SPE Reserv Eval Eng. 1998; 1: 201–206.
3. Palmer I, Mansoori J. How permeability depends on stress and pore pressure in coalbeds: a new model. Proceedings of the SPE Annual Technical Conference and Exhibition; 1996 Oct 6–9; Denver, CO. Calgary: SPE; 1996. doi: 10.2118/36737-MS
4. Kovscek AR, Tang GQ, Jessen K. Laboratory and simulation investigation of enhanced coal bed methane recovery by gas injection. Proceedings of the SPE Annual Technical Conference and Exhibition; 2005 Oct 9–12; Dallas, TX. Calgary: SPE; 2005. doi: 10.2118/95947-MS
5. Karacan CO. Heterogeneous sorption and swelling in a confined and stressed coal during CO_2 injection. Energy Fuels. 2003; 17: 1595–1608. dio: doi: 10.1021/ef0301349
6. Gensterblum Y, Hemert PV, Billemont P. The relationship between permeability and effective stress for Australian coal and its implications with respect to coalbed methane exploration and reservoir model.

Proceedings of the 1997 International Coalbed Methane Symposium. USA University of Alabama. 1997; pp: 13–22.

7. An H, Wei XR, Wang GX. Modeling anisotropic permeability of coal and its effects on CO_2 sequestration and enhanced coalbed methane recovery. International Journal of Coal Geology. 2015; 152: 15–24. doi: 10.1016/j.coal.2015.09.013
8. Kumar H, Elsworth D, Mathers J. Effect of CO2 injection on heterogeneously permeable coalbed reservoirs. Fuel. 2014; 135: 509–521. doi: 10.1016/j.fuel.2014.07.002
9. Alexej M, Yves G, Bernhard M. Competitive sorption of CH_4, CO_2 and H_2O on natural coals of different rank. International Journal of Coal Geology. 2015; 150: 181–192. doi: 10.1016/j.coal.2015.09.006
10. Massarotto P, Golding SD. Changes in reservoir properties from injection of supercritical CO_2 into coal seams—A laboratory study. International Journal of Coal Geology. 2010; 82: 269–279. doi: 10.1016/j.coal.2009.11.002
11. Saikat M, Karl HW. Differential swelling and permeability change of coal in response to CO2 injection for ECBM. International Journal of Coal Geology. 2008; 74: 123–138.
12. Ronny P, Dorian M, Luigi B. Coal characterization for ECBM recovery: Gas sorption under dry and humid condition, and its effect on displacement dynamics. Energy Procedia. 2011; 4: 2157–2161. doi: 10.1016/j.egypro.2011.02.101
13. Sander H, Yves G, Paul M. Sorption and changes in bulk modulus of coal—experimental evidence and governing mechanisms for CBM and ECBM applications. International Journal of Coal Geology. 2014; 128: 119–133. doi: 10.1016/j.coal.2014.04.010
14. Li D, Liu QF, Weniger P. High-pressure sorption isotherms and sorption kinetics of CH4 and CO2 on coals. Fuel. 2010; 89: 569–580. doi: 10.1016/j.fuel.2009.06.008
15. Syed A, Shi JQ, Durucan S. Permeability and injectivity improvement in CO2 enhanced coalbed methane recovery: thermal stimulation of the near wellbore region. Energy Procedia. 2011; 98(4): 2137–2143. dio: doi: 10.1016/j.egypro.2011.02.098
16. Zhou FD, Hou WW, Allinson G. A feasibility study of ECBM recovery and CO_2 storage for a producing CBM field in southwest Qinshui basin, china. International Journal of Greenhouse Gas Control. 2013; 9: 26–40. doi: 10.1016/j.ijggc.2013.08.011
17. Kumar H, Elsworth D, Mathews JP. Effect of CO2 injection on heterogeneously permeability coalbed reservoir. Fuel. 2014; 135: 509–521. doi: 10.1016/j.fuel.2014.07.002
18. Mohammad S, Alireza K. Investigation of varying-composition gas injection for coalbed methane recovery enhancement: A simulation-based study. Journal of Natural Gas Science and Engineering. 2015; 27: 1205–1212. doi: 10.1016/j.jngse.2015.09.071
19. Dutta P, Zoback MD. CO_2 sequestration into the wyodak coal seam of powder river basin-preliminary reservoir characterization and simulation. International Journal of Greenhouse Gas Control. 2012; 9: 103–116. doi: 10.1016/j.ijggc.2012.03.004
20. Sayyafzadeh M, Keshavarz A, Alias ARM, Dong KA, Manser M. Investigation of varying-composition gas injection for coalbed methane recovery enhancement: a simulation-based study. Engineering. 2015; 27: 1205–1212. doi: 10.1016/j.jngse.2015.09.071